Supporting Information: The Transport Mechanisms of Polar Solutes in a Cross-linked H_{II} Phase Lyotropic Liquid Crystal Membrane

Benjamin J. Coscia Michael R. Shirts

December 7, 2018

S1 Water content equilibration

We initially tried to equilibrate our system with water by allowing water molecules to naturally penetrate the membrane from a water bath separating periodic images of the system in the z-direction (See Figure 1a). We allowed a dry, previously equilibrated system to further equilibrate in coexistence with a 3 nm-thick (in the z-direction) layer of water. Water readily enters the tail region where the density of monomers is low. About 3 times more water molecules occupy the tail region after 1000 ns of equilibration (See Figure 1b). Although the water level in the pore appears to plateau in this system, it is clear that equilibration of this system is kinetically limited since water does not fill the pores uniformly. The density of water along the pore axis, averaged over the last 50 nanoseconds of simulation, is close to zero at the membrane center. Therefore, we required a different equilibration technique in order to overcome the kinetic limitation.

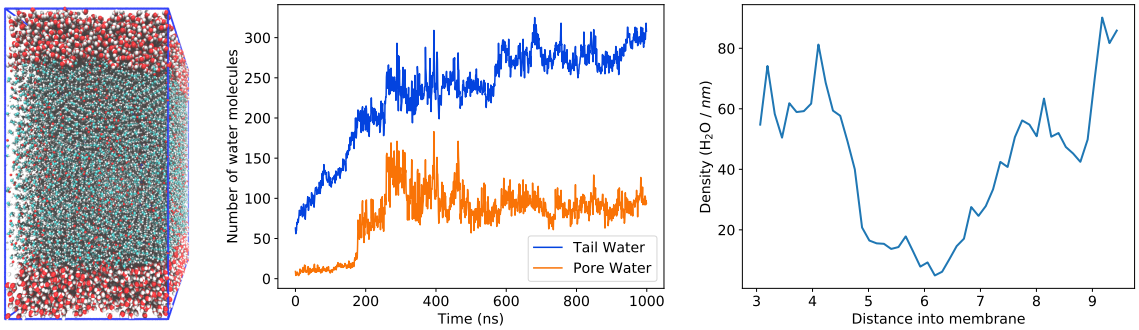

(a) (b) (c)

Figure S1: (a) Using an equilibrated dry configuration, we inserted a layer of water between periodic copies of the system in the z-direction. (b) Water slowly enters the membrane. Most water enters the tail region where the density of monomers is lowest. Water entering the pore plateaus after 500 ns. (c) Although the water content of the pore appears equilibrated in (b), the density of water throughout the pores is not uniform, with almost no water close to the pore center.

We equilibrated 4 systems where we initially placed water in the pores and in the tails along with a water reservoir in between periodic images, much like Figure 1a. We tested a diverse set of systems with varying total water contents and ratios of pore : tail water contents. The intial pore radius dictates the water content of the pore if one is to avoid vacuum gaps. We explored systems with initial pore radii of 5, 6, 7 and 8 Å. Table __ shows the water composition of the pores and the tails for each system studied. In systems started with more water in the tails, the pore water tends to increase over time, while that of the tails decreases or stays stable. Systems started with more water in the pores tend to plateau relatively quickly, with $\sim$ one third of the water staying in the tails.

Pore Radius	wt % water tails	wt % water pores
5	5.67	1.09
6	2.88	2.38
7	1.91	4.12
8	2.78	6.00

Table S1

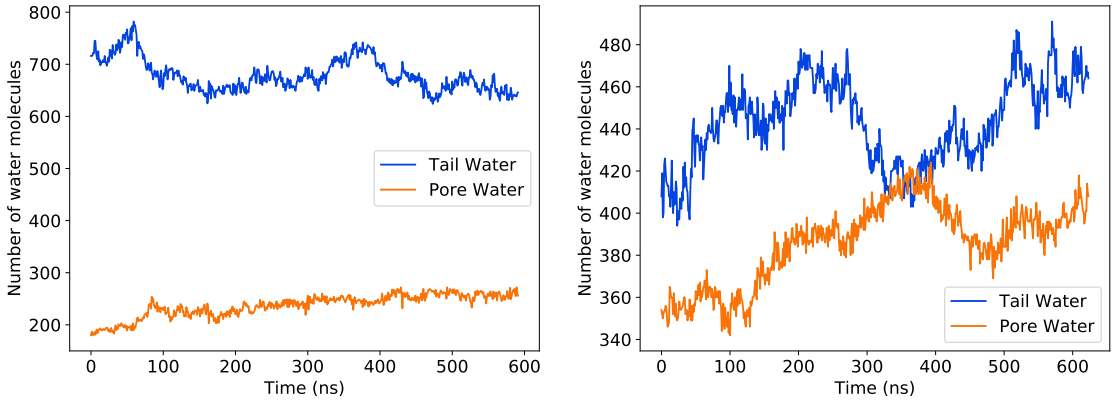

(a) r = 5Å

(b) r = 6Å

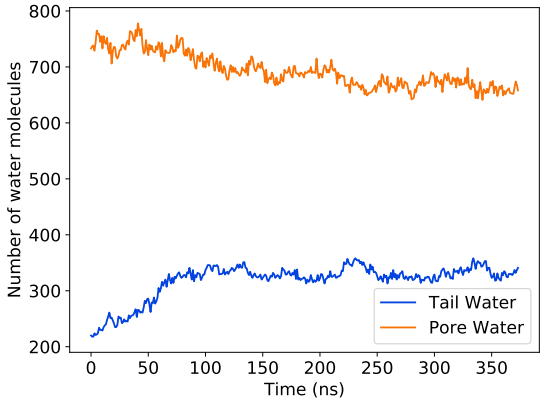

(c) r = 7Å

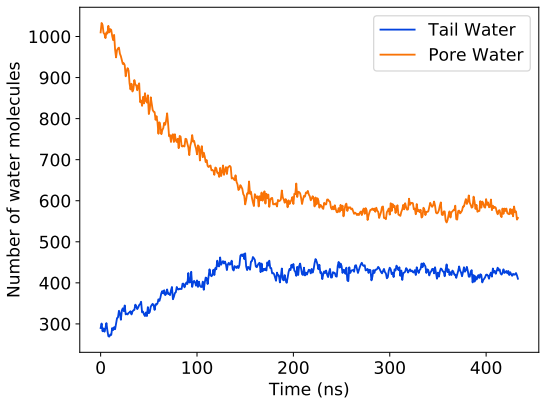

(d) r = 8Å

Figure S2

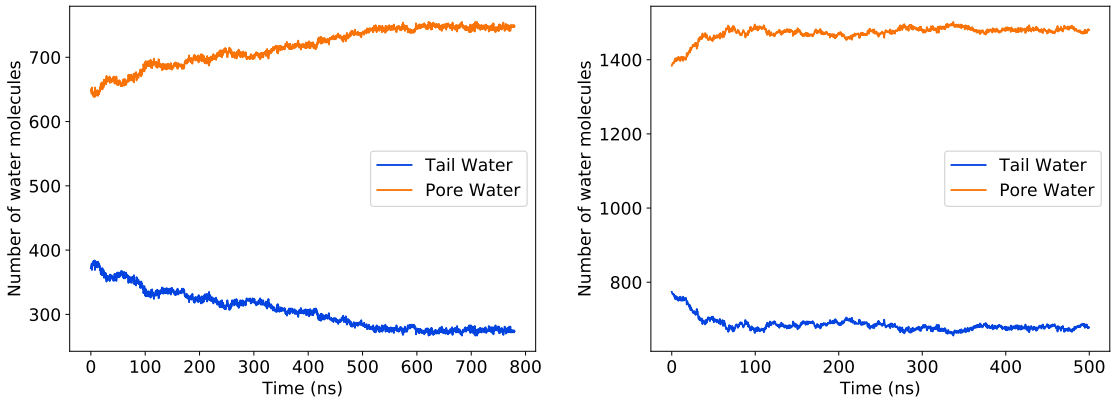

(a) (b)

Figure S3: We created solvated systems with one third of the total water initially placed in the tail region. (a) With 5 wt % total water, the water content equilibrates after 600 ns, with $\sim$ 72 % of the total water in the pores. (b) With 10 wt % total water, the water content equilibrates after 100 ns, with $\sim$ 69 % the total water in the pores.

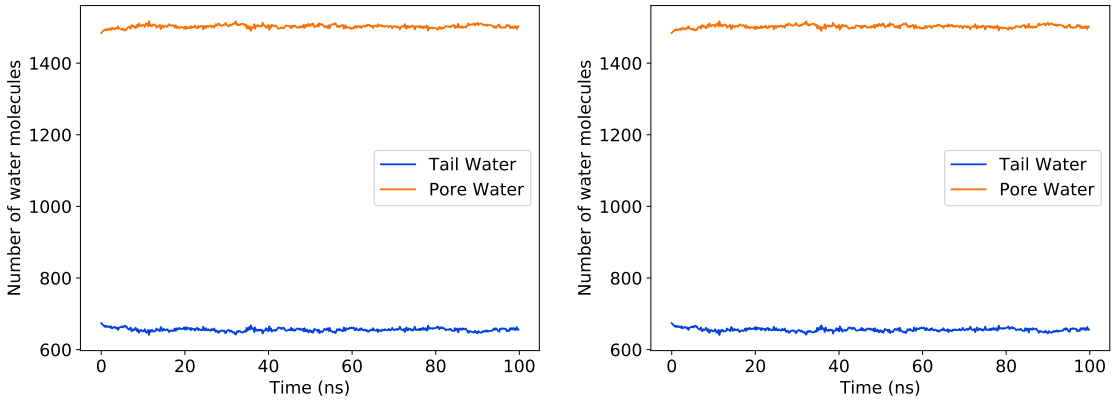

(a) (b)

Figure S4

Since the equilibrium water content is unclear based on the previous simulations, we elected to choose and study systems with two different water contents. We removed the water reservoir and allowed the pore and tail water contents to equilibrate with 5 and 10 wt % water total. We placed one third of the total water needed in the tails. We considered the water content equilibrated once the water contents plateaued. The 10 wt % water system equilibrated within the first 100 ns of simulation, while the 5 wt% system did not plateau until $\sim$ 600 ns (See Figure 4). The pores contain 72 % and 69 % of the total water in the 5 and 10 wt % systems respectively.

We cross-linked the equilibrated solvated systems, then allowed them to equilibrate further for 100 ns.

S2 Choosing a transport model

We used the toolbox created by Meroz and Sokolov in order to justify our choice of transport model.[1] The solutes in our systems exhibit anomalous transport properties characteristic of a Continuous Time Random Walk (CTRW).

Mean Squared Displacement

The general form of a mean squared displacement (MSD) curve is:

$$\langle x^2(t) \rangle \sim t^{\alpha} \tag{1}$$

For brownian motion, $\alpha = 1$ and the MSD is linear. When $\alpha \neq 1$, the particle of interest exhibits anomalous diffusion. Values of α greater than 1 give rise to superdiffusion, while values of α less than 1 give rise to subdiffusion.

We can calculate the ensemble-averaged MSD curve by averaging the MSDs of each particle trajectory, where each MSD is calculated using:

$$\delta^2(t) = \|\mathbf{r}(t) - \mathbf{r}(0)\|^2 \tag{2}$$

where $\| \cdot \|$ represents the Euclidean norm.

The mean squared displacement of solutes in our model is a non-linear function of time, with $\alpha < 1$ which is indicative of anomalous subdiffusion. Figure 5a plots the ensemble-averaged MSD curve for 24 ethanol molecules diffusing in a 10 wt% water H_{II} LLC membrane system. We fit a power law of the form Ae^{α} to the MSD curve. We performed 2000 bootstrap trials by randomly sampling 24 MSD curves with replacement from the 24 total ethanol MSD curves. The bootstrapped average value of α is 0.75 for this system.

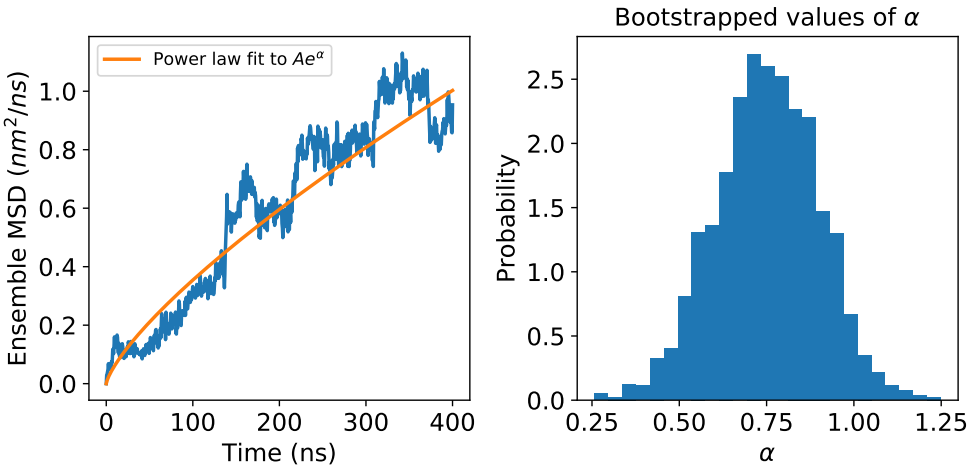

Figure S5: (a) We fit a curve with the form of Equation 1 to the ensemble-averaged MSD curve. (b) The average value of α, obtained using fits to MSDs calculated from bootstrapped ensembles, is less than 1 suggesting that ethanol molecules in our model exhibit subdiffusive behavior.

Ergodicity

The ergodicity of a system can help us narrow down the possible anomalous diffusion mechanisms. In an ergodic system, the time-averaged behavior of an observable should yield the same result as the ensemble average of the same observable. Examples of anomalous diffusion processes that are ergodic include random walks on fractals (RWF) and fractional brownian motion (FBM). Non-ergodic systems generally give rise to CTRWs with the possibility of combination with a RWF and/or FBM.[1]

We tested the ergodicity of our system by comparing the ensemble-averaged and time-averaged MSD curves. We calculated the MSD of each ethanol trajectory using Equation 2 and a time-averaged algorithm:

$$\delta^2(t) = \frac{1}{N-t} \sum_{i=0}^{N-t-1} \|\mathbf{r}(i+t) - \mathbf{r}(i)\|^2 \tag{3}$$

where N is the total number of simulation frames, and t represents the length of subinterval or number of frames per subinterval. We averaged the MSD curves from each trajectory in order to create final MSD plots.

The ethanol molecules exhibit non-ergodic behavior because their time-averaged and ensemble-averaged MSDs do not agree with each other (Figure 6a). We validated our analysis using a 1 ns simulation of a box of tip3p water molecules. As expected, since the particles exhibit Brownian motion, the time-averaged and ensemble-averaged MSDs agree with each within error (Figure 6b).

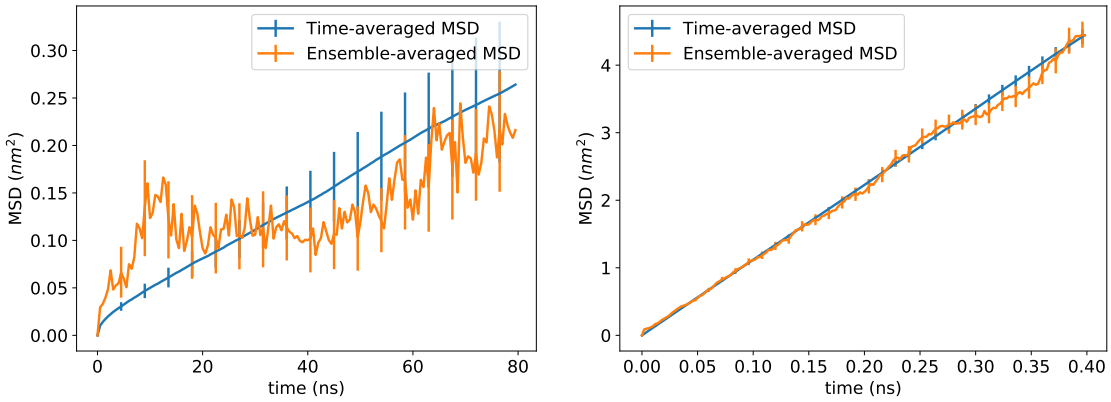

(a) (b)

Figure S6: (a) The time-averaged and the ensemble-averaged MSDs for ethanol in an H_{II} nanopore are not in agreement, implying non-ergodicity. (b) A box of tip3p water molecules is expected to be ergodic and it is shown to be true here because both MSDs are in agreement.

Autocorrelation of steps

Based on the previous two sections, our model can likey be studied as a CTRW. However, it is still possible that our CTRW model might also be convoluted with an FBM or a RWF process. In a pure CTRW, the steps are uncorrelated. Both FBM and RWF exhibit anti-correlated steps.

The steps in our system are not correlated. We showed this by calculating the autocorrelation function (ACF) of the step lengths in the z-direction. The ACF of a representative trajectory is shown in Figure 7.

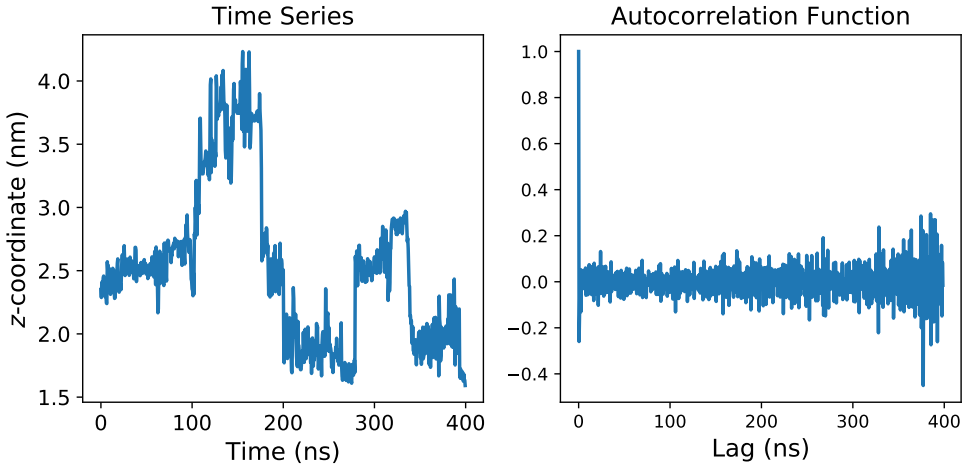

Figure S7: The autocorrelation function (right) of a representative ethanol center of mass z-coordinate trajectory (left) almost immediately decays to zero, indicating a complete loss of memory of it's previous position. Noise increases at large time lags due to decreased sampling.

References

[1] Y. Meroz and I. M. Sokolov, "A Toolbox for Determining Subdiffusive Mechanisms," *Physics Reports*, vol. 573, pp. 1–29, Apr. 2015.